Appl Phys B (2010) 99: 101–106
DOI 10.1007/s00340-009-3819-y

Applied Physics B
Lasers and Optics

Compact fibre-laser-pumped Ho:YLF oscillator–amplifier system

W. Koen · C. Bollig · H. Strauss · M. Schellhorn · C. Jacobs · M.J.D. Esser

Received: 28 July 2009 / Revised version: 3 October 2009 / Published online: 21 November 2009

Abstract We developed a compact Ho:YLF oscillator–amplifier system in a novel setup to utilise the unpolarised pump power from a fibre laser efficiently, and produced 21.3 mJ at 1 kHz, with an M^2 better than 1.1. The amplified energies agreed well with the predicted values from a two dimensional rotational symmetric amplifier model that we developed. The model considers upconversion losses and ground-state depletion, as well as the spatial distribution of the pump beam.

PACS 42.55.Xi · 42.60.Gd · 42.60.Da

1 Introduction

Q-switched lasers operating in the eye-safe 2 μm wavelength region have applications in a number of areas, including remote sensing, defence, materials processing and medical applications. Some of these require reliable and efficient operation in a compact device. Initial work on 2-μm holmium lasers concentrated on thulium–holmium co-doped operation [1]. More recently, work has concentrated on Ho lasers resonantly pumped by Tm lasers, both intra-cavity [2] and extra-cavity [3] pumped. With the emergence of high-power Tm-doped fibre lasers, efficient and robust Ho:YAG lasers pumped by Tm-fibre-lasers were demonstrated [4–6].

However, in order to achieve high-energy Q-switched operation, Ho:YLF is a more attractive laser material than Ho:YAG since it has a much longer upper laser level lifetime (∼14 ms) and higher emission cross section (1.8×10^{-20} cm^2 at 2050 nm versus 1.0×10^{-20} cm^2 at 2091 nm for Ho:YAG) [7, 8]. In addition, the very weak thermal lens on the σ-polarisation helps to deliver diffraction limited beams even under intense end-pumping. However, Ho:YLF has a somewhat stronger quasi-three-level nature than Ho:YAG. In order to reach gain at the 2065 nm line, 22% of the Ho ions need to be pumped into the upper laser level (at room temperature), but it already reaches transparency at the 1940 nm pump wavelength with only 56% of the Ho ions in the upper laser level (see Appendix). In addition, the pump absorption at 1940 nm is relatively weak and strongly polarised. Subsequently, the laser design requires a trade-off between efficient pump absorption and low laser threshold.

Efficient fibre-laser-pumped Ho:YLF oscillators have previously been demonstrated [9], but to scale the output energy further, an oscillator–amplifier system can be employed. The traditional approach when pumping an oscillator–amplifier system with one fibre laser pump source is to split the unpolarised pump beam into two polarised beams in order to pump the oscillator and amplifier crystals separately [10]. In our approach, we use the full unpolarised beam from the fibre laser to pump the oscillator, and then use the partially polarised transmitted pump light from the oscillator to pump the amplifier with its crystal rotated by

W. Koen (✉) · C. Bollig · H. Strauss · C. Jacobs · M.J.D. Esser
National Laser Centre, Council for Scientific and Industrial Research, P.O. Box 395, Pretoria 0001, South Africa
e-mail: wkoen@csir.co.za
Fax: +27-12-8413152

W. Koen
University of KwaZulu-Natal, Durban 4041, South Africa

H. Strauss · C. Jacobs
University of Stellenbosch, Private Bag X1 Matieland, 7602 South Africa

M. Schellhorn
French–German Research Institute, ISL, 5 rue du Général Cassagnou, 68301 Saint-Louis, France

90° around the laser beam axis. This leads to a small system footprint and keeps the path length of the pump light short, reducing adverse effects of water absorption [11].

Figure 1 shows the emission and absorption spectra of Ho:YLF. The emission is stronger on the π-polarisation than on the σ-polarisation. However, the σ-polarisation has a much weaker thermal lens in YLF than the π-polarisation and is thus preferred for a high-power oscillator. In an amplifier, on the other hand, gain is the most important factor while the thermal lens is not as problematic as in an oscillator. Therefore, we chose to utilise the σ-polarisation for the laser oscillator and the π-polarisation for the amplifier.

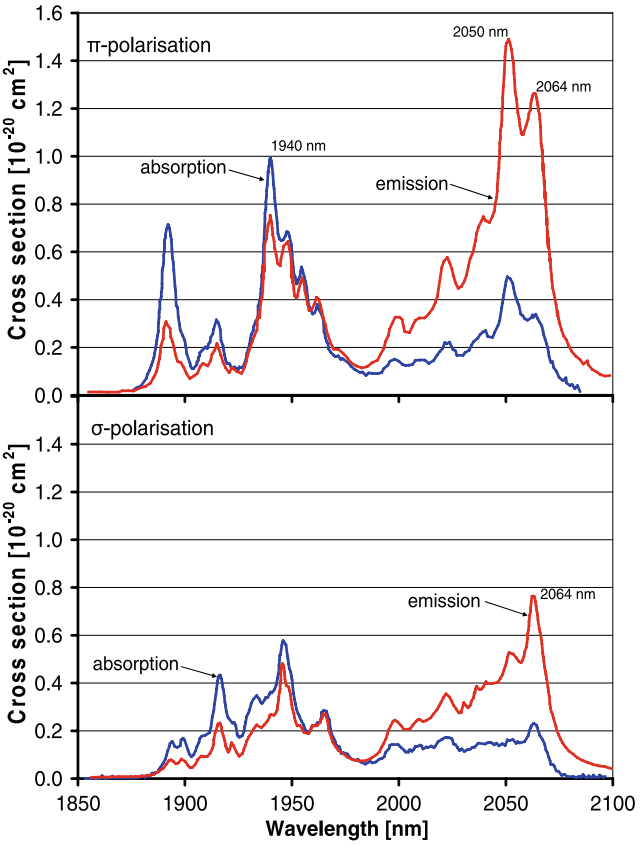

Fig. 1 Ho:YLF absorption and emission cross-sections [8]

2 Experimental set-up

The layout of the Ho:YLF oscillator/amplifier is shown in Fig. 2. A single 82 W Tm-fibre laser (Model TLR-80-1940, from IPG Photonics) was used as pump source. The fibre-laser's wavelength was selected to match the Ho:YLF absorption peak at 1940 nm. The pump light was collimated and sent through a telescope consisting of two lenses with respective focal lengths of 100 mm and −50 mm. The spot radius w_p of the pump beam was measured to be ∼600 µm.

We used the full unpolarised pump beam from the Tm-fibre laser to pump the oscillator crystal, which was a 0.5 at.% doped, a-cut Ho:YLF crystal with a length of 30 mm and a diameter of 6 mm. The crystal was mounted in a water cooled copper mount. The water temperature was kept constant at 20°C. The resonator was 370 mm long with a 500 mm concave back-reflector and a flat output coupler with a reflectivity of 50%. To keep the optical path of the pump light to the amplifier crystal to a minimum, the resonator was folded using 45° dichroic mirrors with high transmission for the pump light (s- and p-polarisation), high reflection for s-polarised laser light, and 20% transmission for π-polarised laser light, forcing the oscillator to operate vertically polarised. Having the c-axis of the crystal horizontal, we insured lasing on the σ-polarisation. A plane cut, AR coated crystal quarts acousto-optic modulator manufactured by *Gooch & Housego* (Model QS027-10M-NL5) was inserted for Q-switched operation. It delivered a loss modulation of approximately 80% at the maximum recommended RF power of 100 W. It was subsequently used with a gate time of 6 µs at 95 W of RF power. Neglecting thermal lensing, the calculated TEM_{00} beam radius in the YLF crystal was 580 µm, which was assumed to increase at higher pump power due to the effect of the weak negative thermal lensing in Ho:YLF.

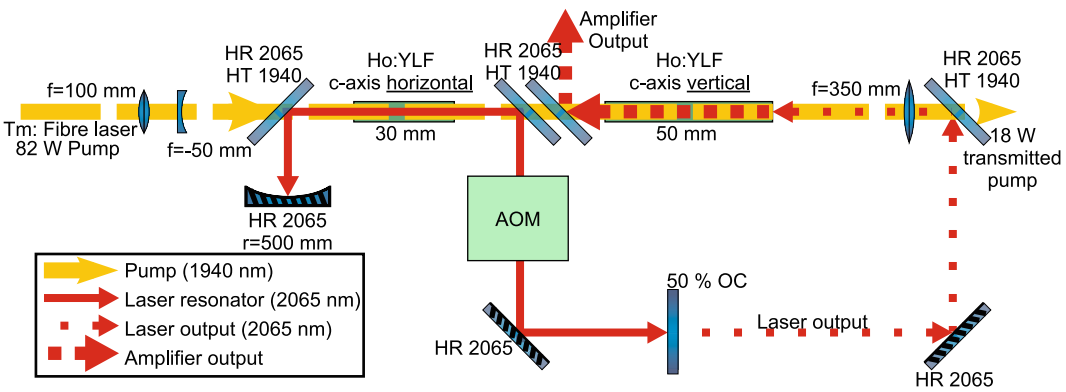

Fig. 2 A schematic diagram of the fibre-laser-pumped Ho:YLF oscillator–amplifier system

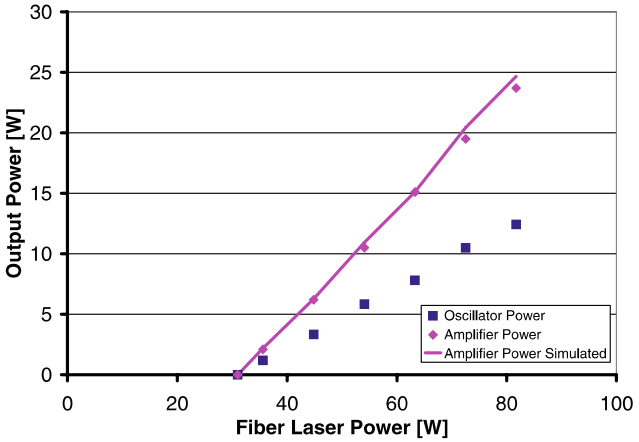

Fig. 3 Oscillator and amplifier output power versus fibre pump power under cw lasing conditions (*data points*) together with the results of a numerical simulation (*solid line*)

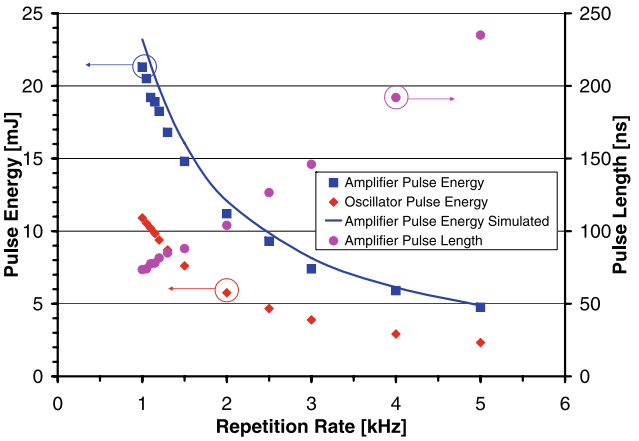

Fig. 5 Oscillator and amplifier output energy and FWHM pulse lengths as a function of the pulse repetition rate at full pump power (*data points*) together with the results of a numerical simulation (*solid line*)

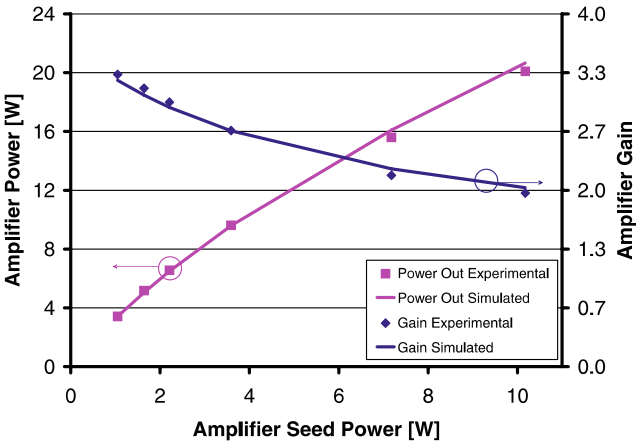

Fig. 4 Amplifier small signal output power and gain under cw operation (*data points*) together with the results of a numerical simulation (*solid lines*)

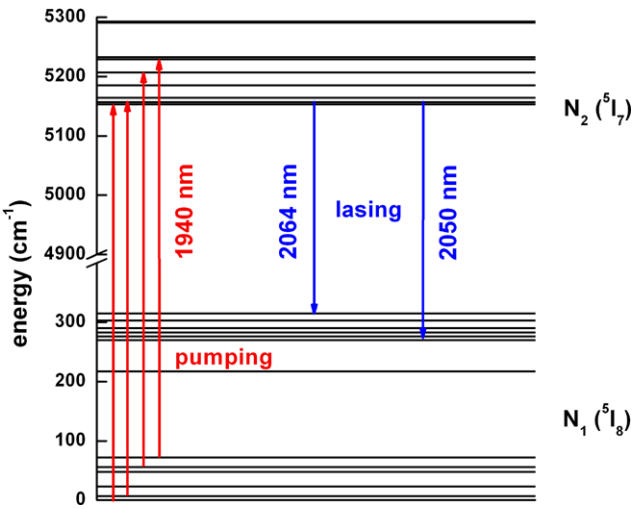

Fig. 6 View of the energy levels of Ho:YLF taken into account in the presented amplifier model [12]

The transmitted pump power was subsequently used to pump the amplifier crystal (50 mm long, also 0.5 at.% doped) which was placed as close to the resonator as possible to minimise atmospheric water absorption of the 1940 nm pump light which would lead to heating of the air and subsequent thermal turbulence. This negated the need for any enclosure or dry-air flushing typically used for such setups to prevent pump-beam distortions caused by thermal turbulence. Since the absorption in Ho:YLF is strongly polarisation dependent, there is a difference between the transmissions of the two polarisations. This makes the transmitted light partially polarised. Therefore, in order to achieve maximum absorption in the amplifier crystal, it was orientated with its c-axis rotated by 90° with respect to the c-axis of the oscillator crystal. This effectively "swapped" the polarisations for the amplifier crystal. Thus, the π-polarisation, with the higher emission cross-section [8] but stronger thermal lens, was used for amplification while the σ-polarisation, with the very weak thermal lens but lower cross section, was used in the oscillator.

The laser output was coupled into the amplifier crystal using a lens with a focal length of 350 mm.

3 Experimental results

The oscillator and amplifier were first operated in cw mode. The output power as a function of the fibre laser pump diode power incident on the crystal is shown in Fig. 3. The oscillator had a threshold of 31 W (17 W absorbed) of pump power, with an overall slope efficiency of 25% (47% vs. absorbed power). At full pump power (82 W), the oscillator power was 12.4 W and the amplified power was 23.7 W at a centre wavelength of 2065 nm. This corresponds to a gain of the

amplifier of 1.9. The total pump power transmitted through the oscillator crystal was 47 W (57% of the pump power) at full power. The amplifier crystal absorbed 62% (29 W) of this transmitted pump light, which left 22% (18 W) of the total pump light unused. The slope efficiency of the amplified beam versus total fibre pump power was 47% with an overall optical-to-optical efficiency of 29%. With respect to the total absorbed power (35 + 29 W), the slope efficiency was 60% and the overall efficiency was 37%. The efficiency with respect to incident pump power could be further increased by reflecting the 18 W transmitted pump light back into the amplifier and oscillator. This was not attempted as it was unclear at the time what the fibre-laser's tolerance to back reflection was.

A two dimensional rotational symmetric amplifier model was developed. The model considers upconversion losses and ground-state depletion, as well as the spatial distribution of the pump and laser beam and is described in detail in the Appendix. The parameter values used in the simulation are listed in Table 1. Taking into account the measured transmitted pump power through the laser crystal, the amplified cw laser power is calculated. The solid line in Fig. 3 shows the results of this calculation which agree well with the experimental values, if we assume a pump and laser spot radius of 550 µm, which is slightly smaller than the measured pump spot at the oscillator crystal of 600 µm. The total upconversion loss constant k_Σ must be set to zero in the simulation. If a small amount of upconversion is considered in the amplifier model (e.g. $k_\Sigma = 1 \times 10^{-18}$ cm^3/s) the gain decreases and the pump and laser spot size must be set to 475 µm to get good agreement with the experimental data, which was not the case in the experiments. Therefore, it can concluded from the amplifier model, that upconversion at the low dopant level of 0.5% in Ho:YLF is negligible.

The amplifier small signal gain was measured under cw operation at a fixed pump power of 75 W of the fibre laser. The oscillator output power was attenuated with different partial reflectors to vary the seed power of the amplifier. The amplifier was pumped with the transmitted pump power of 40 W. Figure 4 shows the measured amplifier small signal output power and gain under cw operation (data points) together with the results of the numerical simulation (solid lines). The results of the simulation show good agreement with the experiment and the small signal gain of ∼3.6 implies that the amplifier is operated nearly in saturation at full cw power.

The oscillator was subsequently Q-switched with an acousto-optic modulator at repetition rates between 5 kHz and 1 kHz. The pulse energies of the oscillator and amplifier and the FWHM pulse lengths as a function of the repetition rate are shown in Fig. 5 at full pump power together with the results of a numerical simulation. Repetition rates below 1 kHz were not attempted in order to keep the intra-cavity energy density below the damage threshold of the 45° pump mirrors. As expected, the highest pulse energies for the system in our operating regime was achieved at a repetition rate of 1 kHz with the oscillator delivering 10.9 mJ per pulse and an amplified pulse energy of 21.3 mJ with a FWHM pulse length of 74 ns. This corresponds to a gain of 2.2. Assuming a pump and laser spot radius of 550 µm (see Table 1) the results of the simulation show good agreement with the experiment and the calculated small signal gain of ∼3.85 at 1 kHz repetition rate is slightly higher than in cw mode. The amplifier did not change the pulse length in any measurable way compared to the oscillator. The beam quality of the amplified beam was measured to be better than an M^2 of 1.1.

Table 1 List of parameter values used in the simulation unless otherwise stated

Description, symbol [unit]	Ho:YLF
Dopant concentration	0.5%
Length of crystal, L [cm]	5
Upper level lifetime, τ_2 [ms] [7]	14
Pump wavelength, λ_p [µm]	1.94
Laser wavelength, λ_l [µm]	2.065
Eff. Stim. em. cross-section, σ_{eff} [10^{-21} cm^2]	12.5
Eff. pump abs. cross-section, σ_{abs} [10^{-21} cm^2]	7
Refractive index, n	1.44
Temperature, T [K]	300
Ratio of Boltzmann factors, F_p	1.2576
Ratio of Boltzmann factors, F_l	0.2845
Pump beam radius, w_p [µm]	550
Super-Gaussian pump parameter, sgp	2
Laser beam radius, w_l [µm]	550
Super-Gaussian pump parameter, sgl	2
Eff. pump quantum efficiency, η_p	1
Total UC loss constant, k_Σ [10^{-18} cm^3/s]	0

4 Conclusion

A novel oscillator–amplifier scheme was developed and successfully demonstrated, where the unused pump light transmitted by the oscillator was utilised to pump an amplifier crystal. The system produced more than 21 mJ energy per pulse at 1 kHz, with an M^2 better than 1.1. The amplified energies agreed well with the predicted values from a two dimensional rotational symmetric amplifier model that we developed. The model considers upconversion losses and ground-state depletion, as well as the spatial distribution of the pump beam. From the good agreement between simulation and experiment it can be concluded that upconversion at

the low dopant level of 0.5% in Ho:YLF is negligible. Further work entails building a single-frequency system with higher output energies at low pulse repetition rates.

Appendix: Amplifier model

We consider a cylindrical amplifier crystal which is end-pumped from one or both sides with a pump laser beam. The beam quality of the fibre laser is excellent ($M^2 < 1.1$). Assuming a spot radius of the pump beam $w_p = 550$ µm the Rayleigh range z_R ($z_R = \pi w_p^2 n/\lambda_p M^2$) is ~640 mm inside the crystal with refraction index $n = 1.44$ (λ_p is the wavelength of the pump beam). Therefore, the amplifier model is treated in a plane wave approximation. For the pump laser, a super-Gaussian intensity distribution is assumed which is given by

$$I_p(r) = \frac{P_p}{\pi w_p^2} \frac{sgp}{2^{1-\frac{2}{sgp}}\Gamma(\frac{2}{sgp})} \exp\left[-2\left(\frac{r}{w_p}\right)^{sgp}\right], \tag{1}$$

where P_p is the pump power, sgp is the super-Gaussian exponent of the pump light and r is the radial position. The launched pump photon density at the entrance surface is thus given by

$$P_{\text{launched}}(r, z = 0) = \frac{I_p(r)n}{c_0 h\nu_p}, \tag{2}$$

where c_0 is the speed of light and $h\nu_p$ is the pump photon energy.

When the YLF amplifier crystal is pumped with the 1940 nm fibre laser, the ground state ions in the $^5I_8$ Ho manifold can be excited to the upper lasing level of the $^5I_7$ Ho manifold as can be seen in Fig. 6. According to [13], the rate equations for the local population densities of the Ho manifolds read as:

$$\begin{aligned}\frac{dN_2(r,z,t)}{dt} = {} & \frac{c_0}{n}\sigma_{\text{abs}}(\lambda_p)\eta_p\left[P^+(r,z,t) + P^-(r,z,t)\right] \\ & \times \left[N_1(r,z,t) - \frac{N_2(r,z,t)}{F(\lambda_p,T)}\right] \\ & - k_\Sigma N_2^2(r,z,t) - \frac{N_2(r,z,t)}{\tau_2},\end{aligned} \tag{3}$$

$$N_1 = N_{\text{tot}} - N_2, \tag{4}$$

where $\sigma_{\text{abs}}(\lambda_p)$ is the absorption cross-sections at the pump wavelength, η_p is the effective pump efficiency of the upper lasing level, P^+ and P^- are the local photon densities of the pump laser fields (the superscripts + and − refer to the forward and backward propagation directions), N_i are the population densities of the Ho ions of manifold i, N_{tot} is the holmium dopant concentration, k_Σ is the total upconversion loss constant [14] and $F(\lambda_p, T)$ is the ratio $(f_1 g_2)/(f_2 g_1)$ of Boltzmann population distributions of Ho, which can be written as [15]

$$F\left(\lambda_p, T\right) = \frac{f_1}{f_2}\frac{g_2}{g_1} = \frac{Z_2(T)}{Z_1(T)} \exp\left[\frac{hc_0}{kT}\left(\frac{1}{\lambda_p} - E_0\right)\right], \tag{5}$$

where $Z_1(T)$ and $Z_2(T)$ are the partition functions of the $^5I_8$ and $^5I_7$ manifolds of Ho as function of the temperature T, and E_0 is the energy of the lowest energy level of the $^5I_7$ Ho manifold.

The forward and reverse propagating pump fields P^+ and P^- are iterated along the length of the amplifier crystal according to

$$\begin{aligned}\frac{dP^\pm(r,z,t)}{dz} = {} & \mp P^\pm(r,z,t)\sigma_{\text{abs}}(\lambda_p) \\ & \times \left[N_1(r,z,t) - \frac{N_2(r,z,t)}{F(\lambda_p,T)}\right].\end{aligned} \tag{6}$$

Note that the negative sign in (6) relates to the forward $(+z)$-direction and the positive sign to the reverse $(-z)$-direction.

The treatment considers either a cw or a Q-switched laser beam to be amplified in a single or double pass through the crystal. For cw, a super-Gaussian intensity distribution is assumed:

$$I_l(r) = \frac{P_l}{\pi w_l^2} \frac{sgl}{2^{1-\frac{2}{sgl}}\Gamma(\frac{2}{sgl})} \exp\left[-2\left(\frac{r}{w_l}\right)^{sgl}\right]. \tag{7}$$

For Q-switching a Gaussian temporal pulse shape according to

$$\begin{aligned}I_l(r,t) = {} & \frac{E_l}{\pi^{3/2} t_0 w_l^2} \frac{sgl}{2^{1-\frac{2}{sgl}}\Gamma(\frac{2}{sgl})} \\ & \times \exp\left[-2\left(\frac{r}{w_l}\right)^{sgl} - \left(\frac{t}{t_0}\right)^2\right]\end{aligned} \tag{8}$$

with

$$t_0 = \frac{t_{\text{FWHM}}}{2\sqrt{\ln(2)}} \tag{9}$$

is assumed, where P_l is the incident laser power (cw mode), E_l is the energy (Q-switched mode) of the incident laser pulse, w_l is the laser spot radius, sgl is the super-Gaussian exponent of the laser light and t_{FWHM} is the full width at half maximum pulse duration of the incident pulse. The launched laser photon density at the entrance surface is therefore given by

$$S_{\text{launched}}(r, z = 0, t) = \frac{I_l(r,t)n}{c_0 h\nu_l}, \tag{10}$$

where $h\nu_l$ is the laser photon energy.

Inside the crystal the forward and reverse propagating amplified laser fields S^+ and S^- (photon densities) are iterated along the length of the crystal according to

$$\frac{dS^{\pm}(r,z,t)}{dz} = \pm S^{\pm}(r,z,t)\sigma_{\text{eff}}(\lambda_l) \times \left[N_2(r,z,t) - F(\lambda_l,T)N_1(r,z,t)\right] + \frac{\Delta\Omega}{4\pi}\frac{N_2(r,z,t)}{\tau_2 c_0}. \quad (11)$$

Note that the positive sign in (11) relates to the forward $(+z)$-direction and the negative sign to the reverse $(-z)$-direction. $\sigma_{\text{eff}}(\lambda_l)$ is the effective stimulated emission cross-section at the Ho wavelength λ_l, $F(\lambda_l, T)$ is the ratio $(f_1 g_2)/(f_2 g_1)$ of Boltzmann population distributions of Ho at the lasing wavelength λ_l given by (5) (by replacing λ_p with λ_l). The last term in (11) is amplified spontaneous emission, where $\Delta\Omega$ is the solid angle given by the length of the amplifier crystal L and the pump spot radius w_p ($\Delta\Omega = 2\pi \cdot (1 - \cos\beta)$, with $\beta = \tan^{-1}(\frac{w_p}{L})$).

Calculating the local population in (3) and iterating (6) and (11) along the length of the amplifier crystal, we obtain the extracted photon densities of the laser field after amplification. The simulations have been done using the parameters listed in Table 1.

A positive gain could be deduced from setting the first term in (11), i.e. $N_2 - F(\lambda_l, T)N_1 > 0$, which results in $N_2/N_{\text{tot}} = F(\lambda_l, T)/(1 + F(\lambda_l, T)) = 0.22$. The amplifier becomes transparent if (6) is set to zero, which results in $N_2/N_{\text{tot}} = F(\lambda_p, T)/(1 + F(\lambda_p, T)) = 0.56$.

References

1. T.Y. Fan, G. Huber, R.L. Byer, P. Mitzscherlich, Spectroscopy and diode laser-pumped operation of Tm,Ho:YAG. IEEE J. Quantum Electron. **24**(6), 924 (1988)
2. C. Bollig, R.A. Hayward, W.A. Clarkson, D.C. Hanna, 2-W Ho:YAG laser intracavity-pumped by a diode-pumped Tm:YAG laser. Opt. Lett. **23**(22), 1757 (1998)
3. P.A. Budni, M.L. Lemons, J.R. Mosto, E.P. Chicklis, High-power/high-brightness diode-pumped 1.9-μm thulium and resonantly pumped 2.1-μm holmium Lasers. IEEE J. Sel. Top. Quantum Electron. **6**(4), 629 (2000)
4. E. Lippert, G. Arisholm, G. Rustad, K. Stenersen, Fiber laser pumped mid-IR source, in *Advanced Solid State Photonics*, ed. by J.J. Zayhowski. OSA Trends in Optics and Photonics Series, vol. 83 (2003), pp. 292–297
5. D.Y. Shen, A. Abdolvand, L.J. Cooper, W.A. Clarkson, Efficient Ho: YAG laser pumped by a cladding-pumped tunable Tm: silica-fibre laser. Appl. Phys. B **79**, 559 (2004)
6. E. Lippert, S. Nicolas, G. Arisholm, K. Stenersen, G. Rustad, Mid-infrared laser source with high power and beam quality. Appl. Opt. **45**, 3839 (2006)
7. S.A. Payne, L.L. Chase, L.K. Smith, W.L. Kway, W.F. Krupke, Infrared cross-section measurements for crystals doped with Er^{3+}, Tm^{3+}, and Ho^{3+}. IEEE J. Quantum Electron. **28**(11), 2619 (1992)
8. B.M. Walsh, N.P. Barnes, B. Di Bartolo, Branching ratios, cross sections, and radiative lifetimes of rare earth ions in solids: Application to Tm^{3+} and Ho^{3+} ions in $LiYF_4$. J. Appl. Phys. **83**(5), 2772 (1998)
9. Y. Bai, J. Yui, M. Petros, P. Petzar, P. Trieu, H. Lee, U. Singh, Highly efficient Q-switched Ho:YLF laser pumped by Tm:fiber laser, in *CLEO/QELS Conference*, paper CtuN5 (2007)
10. A. Dergachev, D. Armstrong, A. Smith, T. Drake, M. Dubois, 3.4-μm ZGP RISTRA nanosecond optical parametric oscillator pumped by a 2.05-μm Ho:YLF MOPA system. Opt. Express **15**, 14404 (2007)
11. L.S. Rothman, A. Barbe, D.C. Benner, L.R. Brown, C. Camy-Peyret, M.R. Carleer, K. Chance, C. Clerbaux, V. Dana, V.M. Devi, A. Fayt, J.-M. Flaud, R.R. Gamache, A. Goldman, D. Jacquemart, K.W. Jucks, W.J. Lafferty, J.-Y. Mandin, S.T. Massie, V. Nemtchinov, D.A. Newnham, A. Perrin, C.P. Rinsland, J. Schroeder, K.M. Smith, M.A.H. Smith, K. Tang, R.A. Toth, J. Vander Auwera, P. Varanasi, K. Yoshino, The HITRAN molecular spectroscopic database: edition of 2000 including updates through 2001. J. Quantum Spectrosc. Radiat. Transfer **82**, 5 (2003)
12. P.L. Cross, Database of laser materials. Laser Systems Branch, NASA Langley Research Center, USA (2004). Previously available from: http://aesd.larc.nasa.gov/gl/laser/dbmain.htm (Accessed March 2005)
13. M. Schellhorn, A. Hirth, Modelling of intracavity-pumped quasi-three-level lasers. IEEE J. Quantum Electron. **38**, 1455 (2002)
14. G. Rustad, K. Stenersen, Modelling of laser-pumped Tm and Ho lasers accounting for upconversion and ground-state depletion. IEEE J. Quantum Electron. **32**, 1645 (1996)
15. R.C. Stoneman, L. Esterowitz, Efficient 1.94-μm Tm:YALO laser. IEEE J. Sel. Top. Quantum Electron. **1**, 78 (1995)